

First measurement of neutrino oscillation parameters using neutrinos and antineutrinos by NOvA

Supplemental Figures

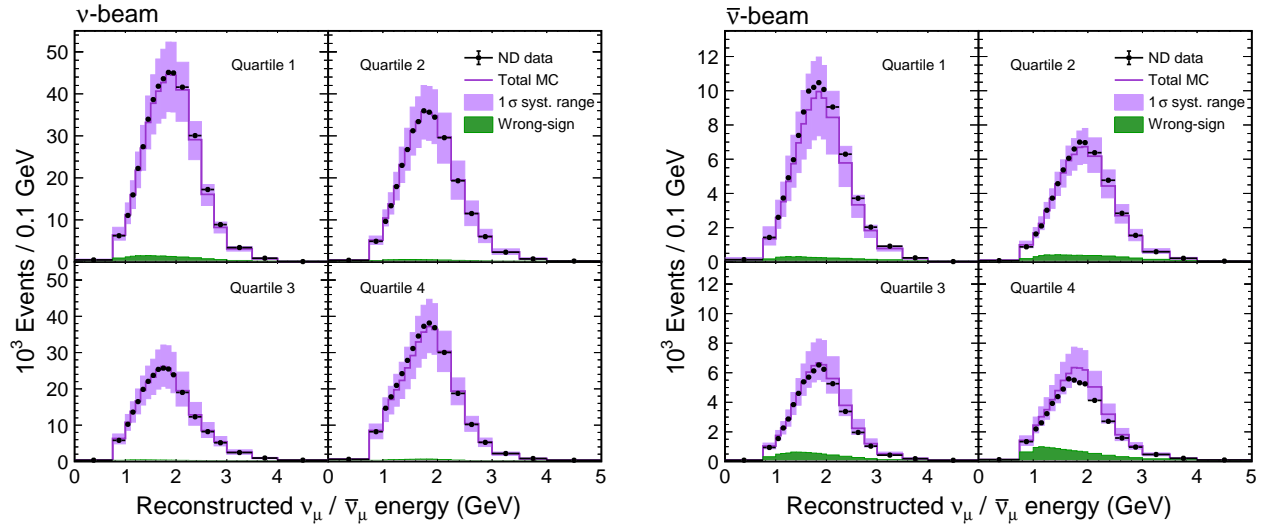


FIG. S1. Reconstructed ν_μ CC energy spectra at the ND shown separately for each quartile of reconstructed hadronic energy fraction, in the neutrino beam on the left and the antineutrino beam on the right. These samples are used to predict the FD ν_μ CC spectra in Fig. S2 below. The spectra are shown with the simulation normalized to the same exposure as the data, and the systematic error band includes all systematic uncertainties.

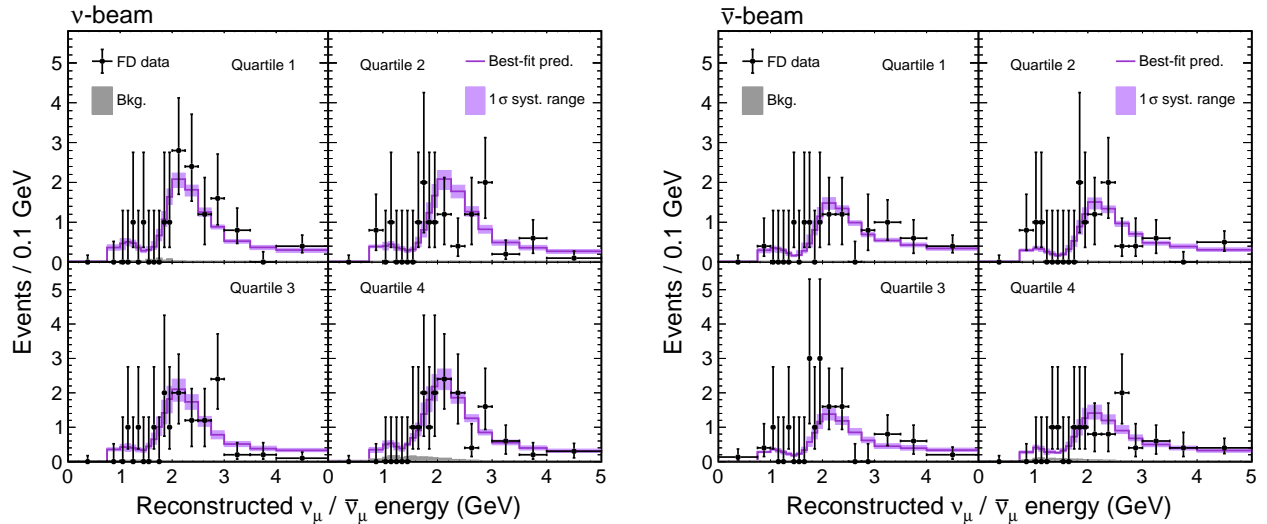


FIG. S2. Reconstructed ν_μ CC energy spectra at the FD shown separately for each quartile of reconstructed hadronic energy fraction, in the neutrino beam on the left and the antineutrino beam on the right. The samples shown here, along with the ν_e CC FD samples in Fig. 1, are fit together to extract the oscillation parameters.

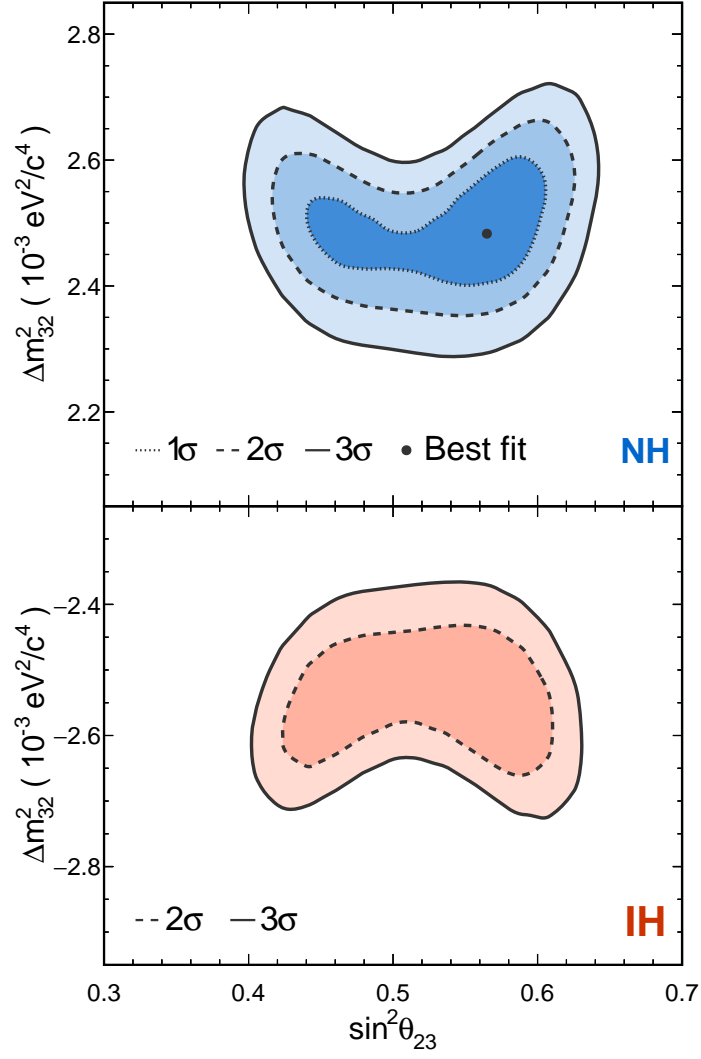


FIG. S3. The 1σ , 2σ , and 3σ contours in Δm_{32}^2 vs. $\sin^2 \theta_{23}$ in the normal hierarchy (NH, top panel) and inverted hierarchy (IH, bottom panel). The best-fit point is shown by a black marker.

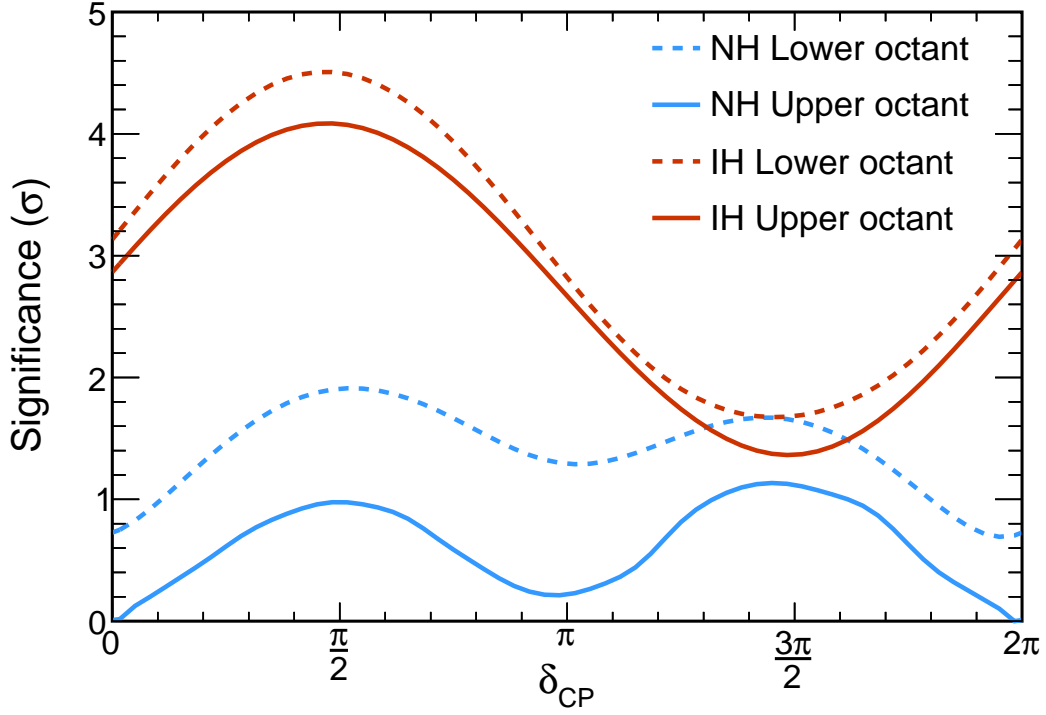


FIG. S4. The projection of the likelihood surface onto the δ_{CP} axis, plotted in terms of significance of rejection of each value of δ_{CP} , under different assumptions of mass hierarchy and the $\sin^2 \theta_{23}$ octant. Zero significance denotes the best-fit point.

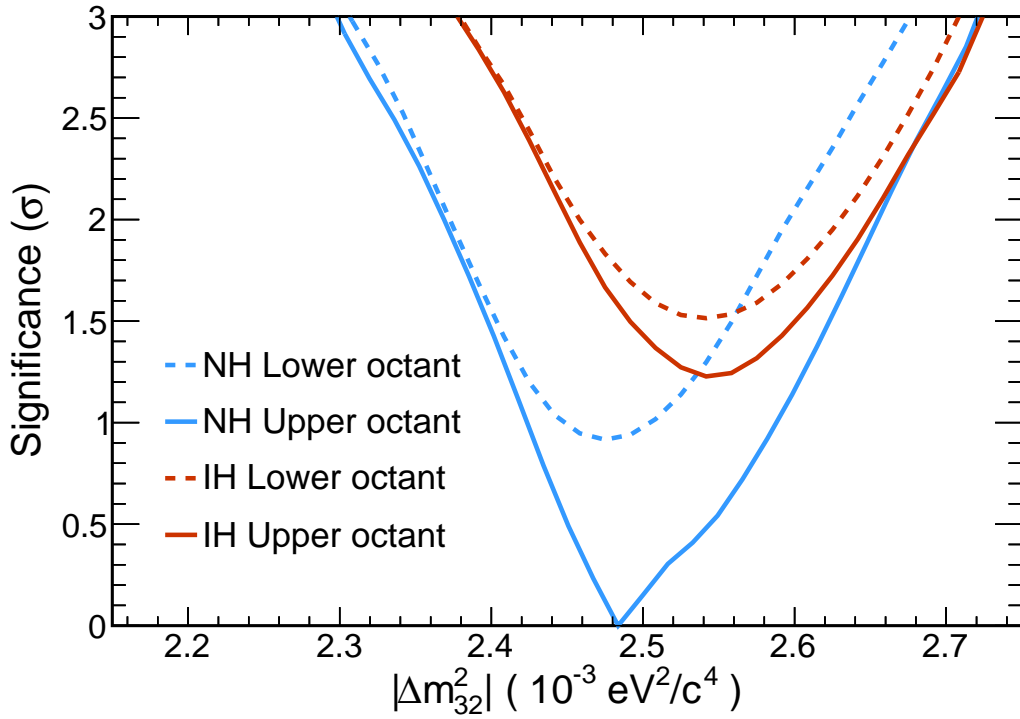


FIG. S5. The projection of the likelihood surface onto the Δm_{32}^2 axis, plotted in terms of significance of rejection of each value of Δm_{32}^2 , under different assumptions of mass hierarchy and the $\sin^2 \theta_{23}$ octant. Zero significance denotes the best-fit point.

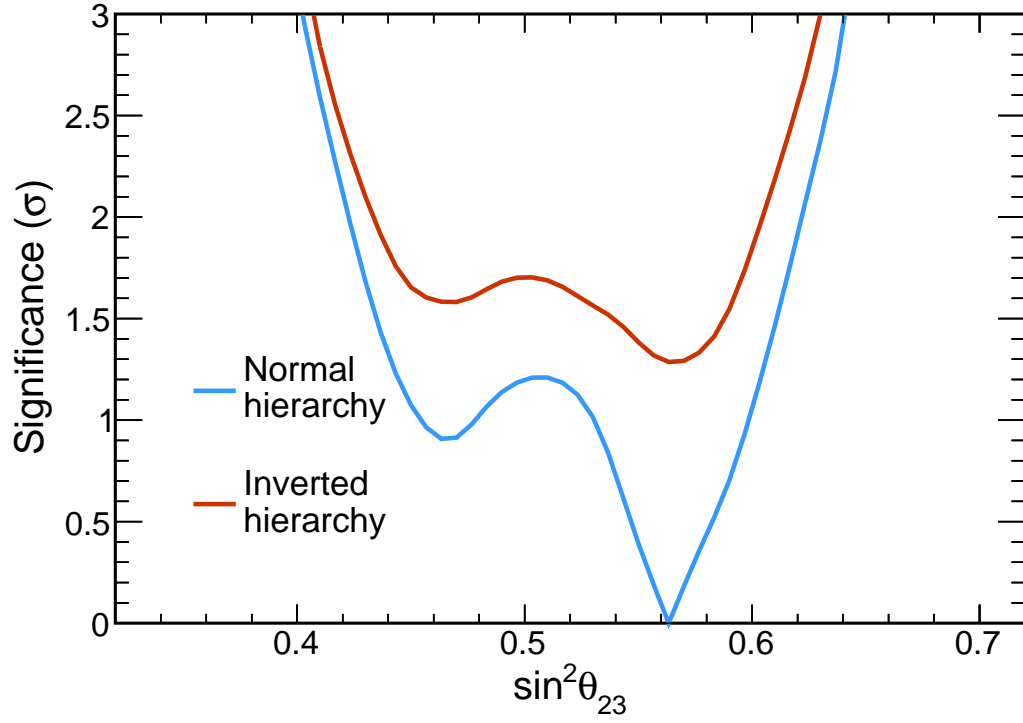


FIG. S6. The projection of the likelihood surface onto the $\sin^2 \theta_{23}$ axis, plotted in terms of significance of rejection of each value of $\sin^2 \theta_{23}$, under different assumptions of mass hierarchy. Zero significance denotes the best-fit point.